0026-895X/06/6902-509–519$20.00
Molecular Pharmacology
Copyright © 2006 The American Society for Pharmacology and Experimental Therapeutics
Mol Pharmacol 69:509–519, 2006

Vol. 69, No. 2
16741/3082567
Printed in U.S.A.

Drug Binding Interactions in the Inner Cavity of hERG Channels: Molecular Insights from Structure-Activity Relationships of Clofilium and Ibutilide Analogs

Matthew Perry, Phillip J. Stansfeld, Joanne Leaney, Claire Wood, Marcel J. de Groot, Derek Leishman, Michael J. Sutcliffe, and John S. Mitcheson

Department of Cell Physiology and Pharmacology, Maurice Shock Medical Sciences Building, University of Leicester, Leicester, United Kingdom (M.P., J.S.M.); Pfizer Global Research & Development, Pfizer Limited, Sandwich, Kent, United Kingdom (J.L., C.W., M.J.d.G., D.L.); and Department of Biochemistry, University of Leicester, Leicester, United Kingdom (P.J.S., M.J.S.)

Received July 14, 2005; accepted November 16, 2005

ABSTRACT

Block of human *ether-a-go-go* related gene (hERG) K^+ channels by otherwise useful drugs is the most common cause of long QT syndrome, a disorder of cardiac repolarization that predisposes patients to potentially fatal arrhythmias. This undesirable long QT side effect has been a major reason for the withdrawal of medications from the pharmaceutical market. Understanding the molecular basis of hERG block is therefore essential to facilitate the design of safe drugs. Binding sites for hERG blockers have been mapped within the inner cavity of the channel and include aromatic residues in the S6 helix (Tyr-652, Phe-656) and residues in the pore helix (Thr-623, Ser-624, Val-625). We used mutagenesis of these residues, combined with an investigation of hERG block by close analogs of clofilium and ibutilide, to assess how specific alterations in drug structure affected potency and binding interactions. Although changing the basic nitrogen from quaternary to tertiary accelerated the onset of block, the IC_{50} and kinetics for recovery from block were similar. In contrast, analogs with different *para*-substituents on the phenyl ring had significantly different potencies for wild-type hERG block. The highest potency was achieved with polar or electronegative *para*-substituents, whereas neutral *para*-substituents had potencies more than 100-fold lower. Results from mutagenesis and molecular modeling studies suggest that phenyl ring *para*-substituents influence drug interactions with Thr-623, Ser-624, and Tyr-652 and strongly affect binding affinity. Together, these findings suggest that modifying the *para*-substituent could be a useful strategy for reducing hERG potency and increasing the safety margin of compounds in development.

hERG (human *ether-a-go-go*–related gene) potassium (K^+) channels mediate the rapidly activating delayed rectifier K^+ current (I_{Kr}) (Sanguinetti et al., 1995) that plays a key role in repolarization of the ventricular action potential (Tseng 2001, Vandenberg et al., 2001). Block of hERG by a wide variety of medications is linked to acquired long QT syndrome, a disorder characterized by lengthening of ventricular action potential duration (represented by an extension of the QT interval on an electrocardiogram), and an increased risk of ventricular arrhythmias and sudden death (Keating and Sanguinetti, 2001). The potential of a drug to cause QT prolongation has been a commonly cited reason for the withdrawal of medications from the pharmaceutical market. As a result, compounds are now subjected to time consuming and expensive screening procedures during development (Fermini and Fossa, 2003; Recanatini et al., 2004). An accurate understanding of the molecular basis of drug binding to hERG would significantly facilitate the development and safety profile of new medications (Sanguinetti and Mitcheson, 2005).

Block of hERG K^+ channels by most drugs requires opening of the activation gate, indicating that compounds bind within the inner cavity (Spector et al., 1996; Mitcheson et al., 2000b). Available evidence suggests hERG has a relatively large inner cavity compared with the K_V channel family (Mitcheson et al., 2000b; Mitcheson and Perry, 2003). Previous studies have used mutagenesis to identify the amino acid

---

This work was supported by grants to J.S.M. from Pfizer Global Research and Development UK and the UK Medical Research Council.

Article, publication date, and citation information can be found at http://molpharm.aspetjournals.org.

doi:10.1124/mol.105.016741.

ABBREVIATIONS: hERG, human *ether-a-go-go* related gene; S6, sixth transmembrane segment; MES, 2-[*N*-morpholino]ethanesulfonic acid; clofilium, 4-chloro-*N*,*N*-diethyl-*N*-heptylbenzenebutanaminium; WT, wild type.

residues lining the inner cavity of hERG that are essential for high-affinity block (Lees-Miller et al., 2000; Mitcheson et al., 2000a). Two aromatic residues on the inner (S6) helix (Tyr-652 and Phe-656) that are unique to the EAG K^+ channel family are critical for binding of most hERG channel blockers (Mitcheson et al., 2000a; Kamiya et al., 2001; Sánchez-Chapula et al., 2002, 2003). Fluvoxamine and dronedarone are examples of drugs in which neither aromatic residue is critical for block (Milnes et al., 2003; Ridley et al., 2004). Nevertheless, most compounds interact with one or both. Mutagenesis studies suggest that an aromatic residue is required at position 652 for high-affinity binding with drugs through either cation-π or π-stacking interactions with charged nitrogen and aromatic groups (Fernandez et al., 2004). In contrast, potency correlates well with hydrophobic indices of residues substituted into position 656 (Fernandez et al., 2004). Gating-dependent positioning of these residues relative to the inner cavity (particularly with inactivation) may be critical for high-affinity binding (Chen et al., 2002) and could explain the higher potency of compounds for hERG compared with EAG block (Herzberg et al., 1998; Ficker et al., 2001).

Three residues at the base of the pore helix (Thr-623, Ser-624, and Val-625), immediately adjacent to the GFG signature sequence of the selectivity filter, have been implicated as potential binding sites for some high-affinity compounds (Mitcheson et al., 2000a; Perry et al., 2004). All three residues are highly conserved in voltage-gated K^+ channels (Shealy et al., 2003). However, their contribution to drug binding (as indicated by shifts in potency with alanine substitutions) is variable when comparing compounds of relatively similar structure (Mitcheson et al., 2000a; Perry et al., 2004). For example, ibutilide and clofilium have few differences in structure and similar potencies for wild-type (WT) hERG block. Nevertheless, marked differences exist in the kinetics of recovery from block and in their sensitivity to mutation of pore helix residues (Perry et al., 2004). In particular, the -fold change in IC_{50} caused by the S624A mutation was much higher for clofilium (381-fold) than for ibutilide (50-fold). Furthermore, the unusually slow recovery from clofilium block observed with WT and most mutant hERG channels was accelerated by the mutation S624A. These results suggested that clofilium formed a specific interaction with Ser-624 and illustrates the importance of pore helix residues for drug binding.

In this study, we used a range of closely related structural analogs of clofilium and ibutilide to investigate the molecular basis for the observed differences in hERG block. Clofilium and ibutilide differ in three ways: 1) the basic nitrogen atom is quaternary in clofilium but tertiary in ibutilide; 2) ibutilide, but not clofilium, contains a benzylic hydroxyl group on the phenyl-amine linker; and 3) the *para*-substituent on the phenyl ring is a chlorine in clofilium and a methanesulfonamide in ibutilide. We demonstrate that the quaternary nitrogen on clofilium confers slow onset of block kinetics. The IC_{50} of the tertiary analog is similar to clofilium. This probably arises because although membrane permeability of the tertiary analog is higher than that of clofilium, mutagenesis studies suggest the inner cavity binding affinity is lower. Drug potency was reduced 100-fold by alterations to the *para*-substituent. Mutagenesis and molecular modeling studies suggest that this is due to less favorable interactions with Thr-623, Ser-624, and Tyr-652.

Materials and Methods

hERG Mutagenesis and Expression in Oocytes. hERG channel mutations were introduced by site-directed mutagenesis (QuikChange; Stratagene, La Jolla, CA), subcloned into the pSP64 expression vector and confirmed by DNA sequencing. Complementary RNA for WT and mutant hERG channel expression in *Xenopus laevis* oocytes was prepared by in vitro transcription using SP6 RNA polymerase (mMessage mMachine kit; Ambion, Austin, TX) after linearization of the hERG construct with EcoRI. Defolliculated oocytes were maintained in culture and injected with cRNA as described previously (Sanguinetti and Xu, 1999).

Voltage Clamp Recordings. The two-microelectrode voltage clamp technique was used to record membrane ionic currents from WT or mutant hERG channels between 1 and 7 days after injection. Currents were recorded at room temperature with a GeneClamp 500B amplifier, digitized at 5 kHz with a Digidata 1322A (Molecular Devices, Sunnyvale, CA), and saved to computer for off-line analysis. Data acquisition and analysis were performed using pClamp8.2 software (Molecular Devices), and further analysis was performed using Prism 4.01 software (GraphPad Software, San Diego, CA). Endogenous chloride currents were attenuated by using a low-chloride extracellular recording solution in which chloride was replaced with MES. The extracellular solution contained 96 mM NaMES, 2 mM KMES, 2 mM $CaMES_2$, 5 mM HEPES, and 1 mM $MgCl_2$, pH adjusted to 7.6 with NaOH. To record currents from hERG channel mutants that exhibit a left shift in the voltage dependence of inactivation (T623A and T623A:S624A), a high-K^+ extracellular solution containing 96 mM KMES and 2 mM NaMES (with all other constituents the same) was used (Mitcheson et al., 2000a). Extracellular solutions were applied from a solution-switching device that allowed the solution outlet barrel to be placed adjacent to the oocyte, directing solution flow around the oocyte (Mitcheson et al., 2000b). This, together with the high flow rate (3 to 4 ml/min), minimized extracellular K^+ accumulation and allowed solution changes in less than 10 s. Microelectrodes were pulled from borosilicate glass using a horizontal micropipette puller (Sutter Instrument Company, Novato, CA) and filled with 3 M KCl, and tips were broken to give resistances of 1 to 2 MΩ.

Protocols and Pharmacology. Clofilium (4-chloro-*N*,*N*-diethyl-*N*-heptylbenzenebutanaminium) tosylate was purchased from Alexis Corporation (Lausen, Switzerland). The clofilium analogs were supplied by Pfizer UK. All compounds were dissolved in dimethyl sulfoxide to produce 10 mM stocks and stored at −20°C. On the day of the experiment, drug stocks were diluted to the required concentration in the appropriate extracellular solution. Unless otherwise stated, the protocol used to assess hERG drug block was performed by applying a 5-s depolarizing pulse from a holding potential of −90 to 0 mV before measuring peak tail current amplitude upon repolarization to −70 mV for 400 ms. Before drug application, oocytes were repetitively depolarized every 6 s until current amplitudes were stable over 10 pulses. Repetitive depolarizing pulses were then applied in the presence of drug until steady-state block was reached. This protocol ensures the channels are in the open-inactivated conformation for the majority of the time. Leak subtraction was performed by stepping briefly to −70 mV from the holding potential and subtracting the resulting leak current from the peak hERG channel tail currents. Currents after drug addition were normalized to control ($I_{Drug}/I_{Control}$). The concentration of drug that achieved half-maximal inhibition (IC_{50}) was obtained by fitting data with a Hill function, $I_{Drug}/I_{control} = 1/(1 + ([D]/IC_{50})^{n_H})$, in which [D] and n_H correspond to the drug concentration and Hill coefficient, respectively.

Current-voltage relationships were generated by applying 5-s depolarizing pulses from a holding potential of −90 mV, to potentials between −60 and +50 mV in 10-mV increments, with tail currents measured at −70 mV. The half-point ($V_{0.5}$) and slope factor (k) for the voltage dependence of activation were obtained by fitting peak tail current-voltage relationships with a Boltzmann function. Current reversal potential and deactivation kinetics were determined from tail currents at potentials between +30 and −140 mV after 1-s depolarization to +30 mV to fully activate hERG currents. Time constants for deactivation were obtained by fitting tail current decay with exponential functions. Data are presented as mean ± S.E.M., and n refers to the number of oocytes. Statistical analysis to compare biophysical properties and blocking potency of mutant to wild-type hERG channels were performed using either analysis of variance tests with Dunnett's comparison or Student's t test (as indicated). Differences were considered significant for $P < 0.05$.

Homology Modeling. A homology model of hERG was created using Modeler 6 (Sali and Blundell, 1993), with KcsA [Protein Data Bank (Berman et al., 2000) code 1bl8; Doyle et al., 1998] as the template structure. Ten homology models were generated, with the lowest energy model selected. To eliminate the effects of residues Ser-649 and Ser-660—because mutagenesis seems to preclude their involvement in drug binding (Perry et al., 2004)—the S6 transmembrane helices of the model were rotated slightly, using the Yale Morph Server (http://www.molmovdb.org/morph/), so that these two serine residues are displaced from the binding site—thus preventing them from influencing ligand binding—whereas the aromatic residues remain exposed to the binding site. This approach will be described in detail elsewhere (P. J. Stansfeld, P. Gedeck, J. S. Mitcheson, and M. J. Sutcliffe, manuscript in preparation). Sybyl 6.8 (Tripos Inc., St. Louis, MO) was used to build the ligand structures. Drug dockings were performed using GOLD (Jones et al., 1997), without restraints, with a sphere radius of 20, and with an origin central to the cavity. The ligand dockings were scored based on the parameters of the GoldScore function, with the top 10 binding modes retained. hERG-ligand complexes were visualized using Pymol (http://www.pymol.org).

Results

Comparison of Quaternary Clofilium with a Tertiary Analog. Ibutilide and clofilium are ammonium salts that share similar core structures consisting of a phenyl ring, a four-carbon linker to a central nitrogen, and a seven-carbon aliphatic tail. Despite their similar potency, they exhibit different recovery from block kinetics and binding site interactions within the inner cavity of hERG (Perry et al., 2004). One potentially important structural difference between these two compounds is that clofilium is a quaternary ammonium salt, whereas ibutilide is a tertiary compound. The tertiary central nitrogen on ibutilide allows the compound to exist in a neutral or protonated (positively charged) state at physiological pH. By contrast, the quaternary central nitrogen on clofilium carries permanent positive charge that confers low lipid permeability and is thought to be responsible for its slow equilibration across the plasma membrane and slow kinetics for hERG block (Castle 1991; Gessner and Heinemann, 2003). To determine whether the extra ethyl group on the central nitrogen (and permanent positive charge) is responsible for the distinct kinetics and/or binding of clofilium, we compared block by a tertiary analog PNU-0068611A (structures given in Fig. 1A).

Representative WT-hERG current traces before (control) and after steady-state block by clofilium and PNU-0068611A are shown in Fig. 1B, i and ii, respectively. Both compounds blocked WT-hERG with similar high-affinity (Fig. 1C). The IC_{50} of PNU-0068611A was 80.84 ± 20.8 nM ($n = 4$) (Fig. 1C), which compares with an estimated IC_{50} of 30 nM for clofilium (Perry et al., 2004). As discussed previously (Perry et al., 2004), the IC_{50} for clofilium is difficult to precisely

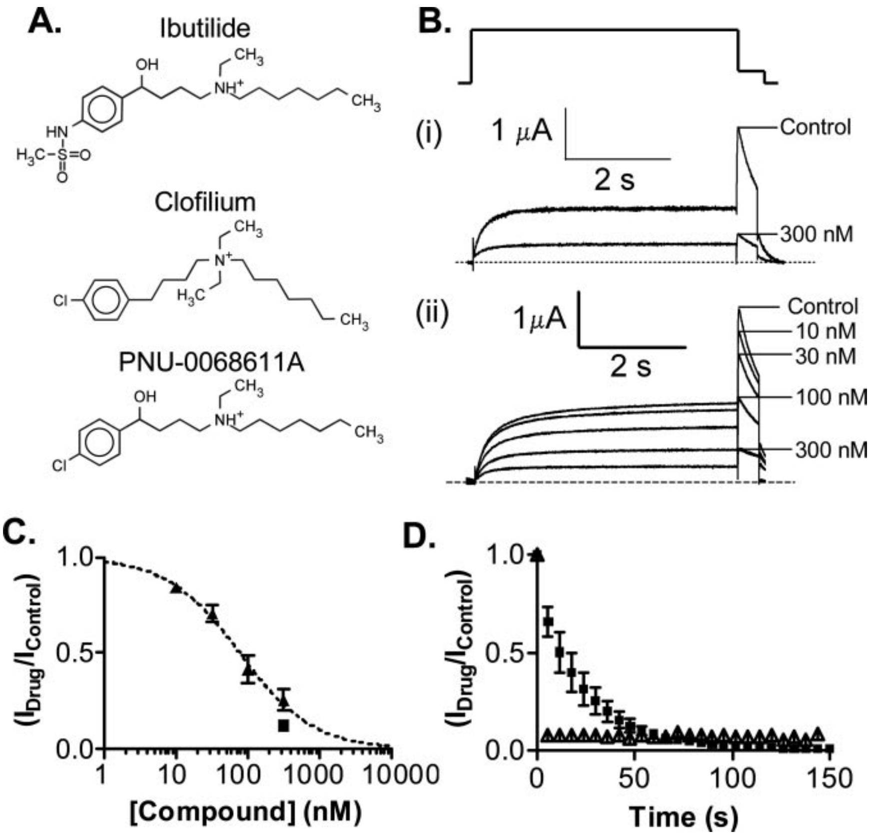

Fig. 1. Comparison of WT-hERG block by clofilium and the tertiary compound PNU-0068611A. A, chemical structures of ibutilide, clofilium, and PNU-0068611A. B, outward currents (zero current shown by dashed line) recorded from WT-hERG expressed in *X. laevis* oocytes. Protocol duration was 6 s, with a 5-s depolarization to 0 mV from a holding potential of −90 mV and peak tail current measured upon repolarization to −70 mV for 400 ms (top). Representative steady-state currents obtained after repetitive pulses before (control) and after addition of 300 nM clofilium (i) and 10, 30, 100, and 300 nM PNU-0068611A (ii). C, concentration-response relationship for block of WT-hERG tail current by clofilium (■) and PNU-0068611A (▲). Mean IC_{50} values are 80.84 ± 20.8 nM ($n = 6$) for PNU-0068611A and were estimated at ~30 nM for clofilium. D, comparison of time-dependent block of WT-hERG by 10 μM clofilium (■) and PNU-0068611A (▲). Peak tail current measured after each test pulse to 0 mV in the presence of drug was normalized to the control current.

measure because of the extraordinarily slow time course for onset of block with low (< 100 nM) concentrations (Gessner and Heinemann, 2003; Perry et al., 2004). Percentage block with 300 nM was slightly greater for the quaternary than tertiary compound. There were, however, very significant differences in the rates of onset of block. Steady-state block by PNU-0068611A occurred within a single pulse (Fig. 1D). Fitting with a single exponential function produced mean time constants for the onset of block of 2.14 ± 0.37s ($n = 4$) and 23.11 ± 0.46s ($n = 4$) for PNU-0068611A and clofilium (10 μM each), respectively ($P < 0.005$, unpaired t test). These findings clearly demonstrate that the permanent positive charge of clofilium is responsible for the slow onset kinetics. Other tertiary analogs of clofilium (see Fig. 4), without the benzylic hydroxyl group of PNU-0068611A, also exhibit rapid block, suggesting that the hydroxyl group does not contribute significantly to the kinetics of block by PNU-0068611A.

Alanine scanning mutagenesis has previously been used to identify several residues at the base of the pore helices (Thr-623, Ser-624, Val-625) and on S6 helices (Gly-648, Tyr-652, Phe-656, Val-659) that are required for high affinity block by ibutilide and clofilium (Perry et al., 2004). However, the increase in IC_{50} (representative of decreased affinity) with each alanine mutation varied between the two compounds, suggesting different binding conformations. To examine whether the quaternary amine of clofilium mediated these effects, we compared block of pore helix and S6 helix mutants by clofilium and the tertiary analog PNU-0068611A. A positive shift in the voltage dependence of activation or dramatic slowing of deactivation can contribute to a decrease in sensitivity to drug block. The mean slope (k), half-maximal point of activation ($V_{0.5}$) and time constants for deactivation of WT and mutant hERG channels are given in Table 1. Only the S624T mutation produced a significant shift in $V_{0.5}$ of activation compared with WT-hERG (−17.3 ± 0.8 mV for S624T versus −22.4 ± 1.6 mV for WT-hERG; $P < 0.01$ one-way analysis of variance). S624A time constants of deactivation were statistically significantly slower ($P < 0.05$) than WT. However, neither change is likely to be sufficient to significantly alter sensitivity to block.

To investigate the relative importance of pore helix residues in drug binding and to determine whether interactions with the quaternary amine are required for clofilium block,

TABLE 1

Mean (± S.E.M.) activation and deactivation properties of hERG channel mutants

Measurements were taken from current-voltage relationships. Fitted with a Boltzman sigmoidal function to give the potential of half-maximal activation ($V_{0.5}$) and the slope of the activation curve. Time constants for fast (τ_{fast}) and slow (τ_{slow}) deactivation were obtained by fitting tail current decay at −70 mV with double exponential functions. $n \geq 5$ for all parameters.

	Activation		Deactivation	
	$V_{0.5}$	k	τ_{fast}	τ_{slow}
	mV		ms	
Wild-type	−22.4 ± 1.5	8.2 ± 0.13	231 ± 5	1065 ± 32
S624A	−24.2 ± 0.7	8.2 ± 0.28	391 ± 19**	1549 ± 70**
S624T	−17.3 ± 0.8**	8.1 ± 0.26	290 ± 13*	1059 ± 71
T623A	−24.2 ± 0.9	5.4 ± 0.18*	208 ± 3**	635 ± 63**
T623A:S624A	−23.4 ± 0.6	7.3 ± 0.15	183 ± 12**	532 ± 32**

* Significance relative to WT hERG of $P < 0.05$.
** Significance relative to WT hERG of $P < 0.01$.

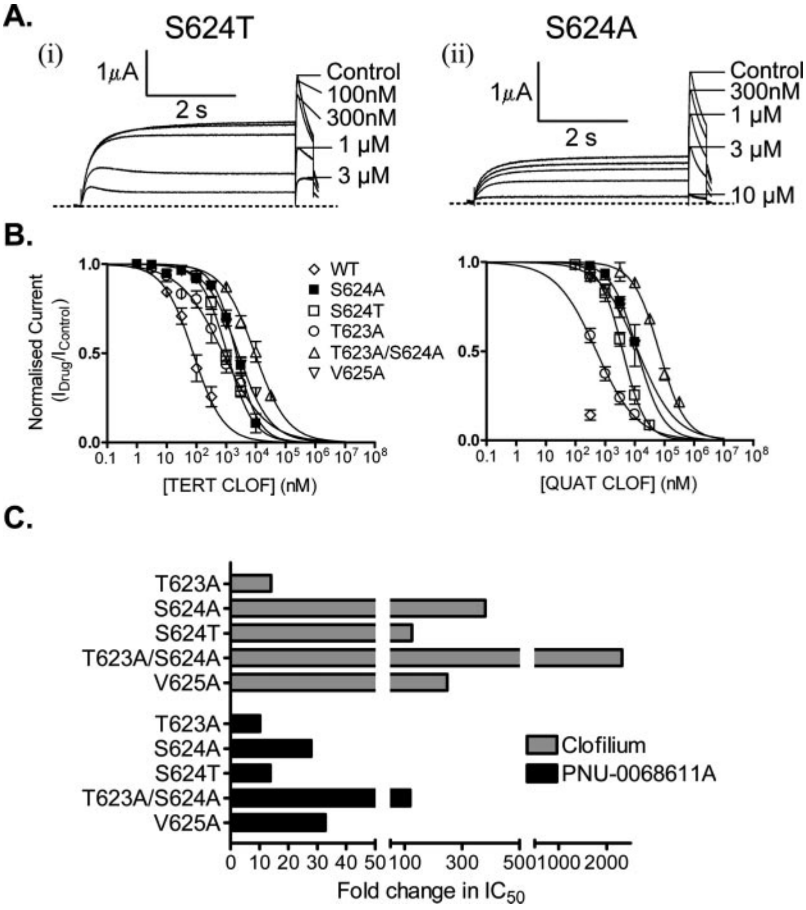

Fig. 2. Concentration dependent block of pore helix mutant hERG channels expressed in *X. laevis* oocytes. A, representative steady-state currents obtained from S624T (i) and S624A (ii) hERG channels after repetitive pulses before (control) and after the addition of increasing concentrations (as indicated) of PNU-0068611A. Note the significantly slowed deactivation observed with 3 μM PNU-0068611A, which may be due to recovery from block during the tail pulse to −70 mV. B, concentration-response relationships for block of hERG channel currents by PNU-0068611A (left) and clofilium (right). IC_{50} values are given in Table 3. C, summary of -fold changes in IC_{50} values for each pore helix hERG mutant compared with WT-hERG.

tertiary analogs and clofilum were applied to alanine mutants, and the effects on IC_{50} were measured relative to WT hERG. Figure 2A shows typical S624T (i) and S624A (ii) hERG currents before (control) and during exposure to increasing concentrations of PNU-0068611A. All pore helix mutant channels exhibited decreased sensitivity to block by both compounds (Fig. 4B). The rank order of importance for mutations that decrease binding affinity was T623A:S624A > V625A > S624A > S624T > T623A for PNU-0068611A and T623A:S624A > S624A > V625A > S624T > T623A for clofilium. For both compounds, the greatest -fold shift in IC_{50} was observed with the double T623A:S624A mutation, with smaller shifts for the single mutants (Fig. 2C). Therefore, interactions with the remaining polar residue may compensate, to some extent, for loss of energetically favorable interactions arising from the mutation. Both analogs have a greater affinity for Ser-624 than with Thr-623, suggesting that the spatial positioning of the hydroxyl group of Ser-624 is more optimal than with Thr-623. Indeed, the conserved mutation S624T reduced, but did not abolish, the loss of sensitivity to block observed with the S624A mutation, indicating the importance of appropriate positioning of the hydroxyl group. It is noteworthy that high concentrations of clofilium and the tertiary analog caused an apparent slowing of S624T hERG deactivation (Fig. 2A). This phenomenon was probably due to recovery from block upon repolarization and was not observed in S624A or other mutant channels, which suggests a reduction of binding affinity upon channel deactivation. A transient component of current caused by the re-onset of block can be seen at the beginning of the test pulses (Fig. 2A, i).

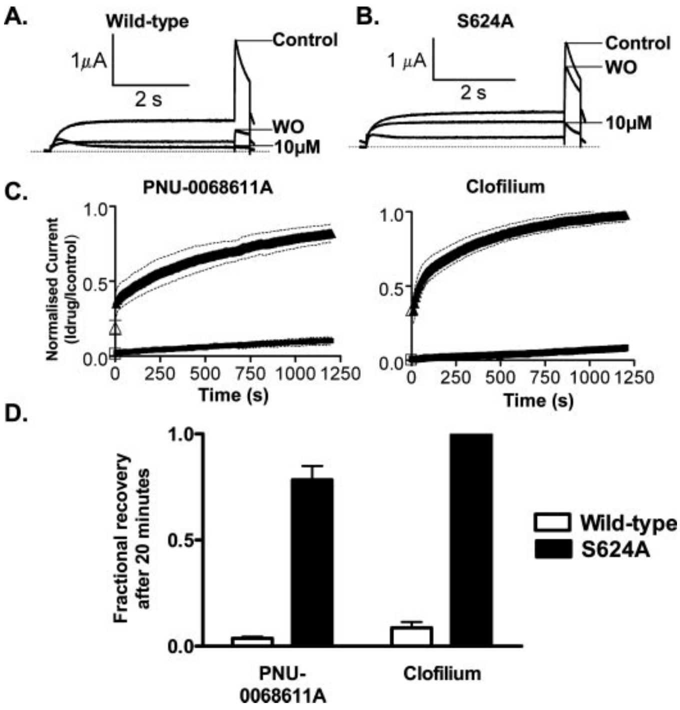

Fig. 3. Rate of recovery from block of WT and S624A mutant hERG channels. A and B, representative steady-state current traces from WT (A) and S624A mutant (B) hERG channels. Currents are shown before drug addition (control), after steady-state block by 10 μM PNU-0068611A, and 20 min after wash-out of the drug (WO). Note the greater recovery from block of S624A channels compared with WT-hERG. C, mean time course for recovery from block of WT and S624A hERG by 10 μM PNU-0068611A (left) and clofilium (right). Open symbols show steady-state block of tail currents from WT (□) and S624A (△) hERG. Closed symbols show mean peak tail currents during each repetitive pulse over a 20-min period of wash-off. D, summary of the fractional recovery from block after 20 min of drug wash-off. Calculated as $(I_{drug} - I_{wash\text{-}off})/(I_{control} - I_{drug})$.

Very slow recovery from block is a feature of clofilium (Fig. 5A) and is likely to contribute to its high potency. Clofilium recovery from block is much slower than ibutilide, and we have shown previously that this is due to differences in binding interactions rather than drug trapping (Perry et al., 2004). To test whether the quaternary amine group is required, we investigated recovery from block of the tertiary clofilium analog. WT-hERG current was inhibited by >95% by 10 μM PNU-0068611A. After removal of drug from the recording solution and with continuous repetitive pulsing to 0 mV for 20 min, only minimal (<5%) recovery from block was observed (Fig. 3C), similar to clofilium. Thus, the quaternary amine is not responsible for this property. In contrast, recovery from block of S624A hERG by PNU-0068611A and clofilium was rapid (Fig. 3C). Mean values for recovery from block after 20 min, expressed as a percentage of initial steady-state block, were 99.6 ± 0.2% and 78.4 ± 6.5% for clofilium and PNU-0068611A, respectively (Fig. 3D). Thus, the slow recovery from block is dependent on Ser-624 and does not require the quaternary amine of clofilium.

Both PNU-0068611A and clofilium exhibited a similar pattern of shifts in IC_{50} for the pore helix mutants, suggesting that they share the same binding sites on this region of the channel. However, the size of the shifts in IC_{50} for all pore helix mutants was much greater for the quaternary compound (see Fig. 2C), suggesting that more favorable interaction energies compared with the tertiary analog. For S6 mutants (Y652A and F656A) the pattern was different (Fig. 4). Although F656A shifted IC_{50} for both compounds by similar amounts (484- and 420-fold for clofilium and PNU-0068611A,

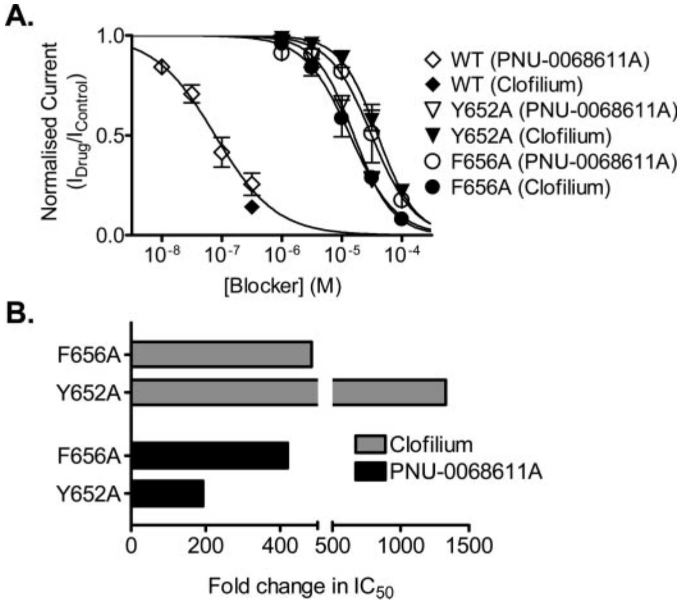

Fig. 4. Y652A and F656A mutations decrease affinity of hERG to clofilium and the tertiary compound PNU-0068611A. A, concentration-response relationships for block of hERG tail currents by clofilium and PNU-0068611A. B, summary of -fold changes in IC_{50} values for each S6 helix hERG mutant compared with WT-hERG. IC_{50} values are given in Table 3.

respectively), the shifts were markedly different for Y652A (1329-fold for clofilium and 193-fold for PNU-0068611A). These findings indicate a stronger interaction with Tyr-652 for clofilium than PNU-0068611A, for which there are several possible explanations. First, the addition of a hydroxyl group one carbon from the phenyl ring on PNU-0068611A may alter its electrostatic potential and decrease the affinity of the π-stacking interaction with Tyr-652. Second, the removal of an ethyl group from the central nitrogen would remove its permanent positive charge and decrease the affinity of the cation-π interaction with Tyr-652. However, this seems unlikely given that the predicted pK_a is 9.96; therefore, >99% of PNU-0068611A molecules are predicted to be protonated. On the other hand, removal of an ethyl group may reduce hydrophobic interactions with Tyr-652, as suggested by our docking studies. Third, removal of an ethyl group and/or the addition of the hydroxyl group may allosterically alter the positioning of the compound within the inner cavity, thereby decreasing its ability to interact at one or more binding sites. Some evidence for this comes from a three-dimensional quantitative structure-activity relationship pharmacophore study in which a decrease in volume around the lower region of the phenyl ring (equivalent to loss of hydroxyl group) or an increase in volume around the central nitrogen (equivalent to the addition of an ethyl group) increased pharmacophore activity (Cavalli et al., 2002). The increased interaction of clofilium with Tyr-652 would presumably also stabilize the drug to enable optimum interactions of the *para*-substituent with pore helix residues.

Effect of Changing the *para*-Substituent on the Phenyl Ring. Another important difference between ibutilide and clofilium is in the nature of the *para*-substituent attached to the phenyl ring, which is a methanesulfonamide in ibutilide and a chlorine in clofilium (see Fig. 1A). Mutagenesis and modeling data so far suggests that the *para*-substituent interacts with polar residues (Thr-623 and Ser-624) at the base of the pore helix (Perry et al., 2004). If this is the case, specific changes in the nature of the *para*-substituent would be expected to alter compound potency and influence the relative shifts of IC_{50} caused by pore helix mutations. To test this hypothesis, we compared PNU-0068611A with three analogs in which nitro, amine, or amide groups replaced the chlorine (structures shown in Fig. 5, A–C). In WT-hERG, IC_{50} values varied by more than 100-fold. The rank order of potency was nitro > chlorine > amine > amide, with IC_{50} concentrations of 2.51 ± 0.4 (n = 5), 80.8 ± 20.8 (n = 4), 273.2 ± 16.8, and 328.7 ± 91.2 nM, respectively. The identity of the *para*-substituent clearly has dramatic affects on potency. This is not a feature of clofilium analogs alone. Altering the *para*-substituents of dofetilide (Table 2) also affects potency. Thus, despite the fact that UK-068522 and UK-068097 have identical core structures (i.e., the same central nitrogen, linkers, and number of cyclic carbon rings), differences in the *para*-substituents resulted in these compounds being 54- and 20-fold less potent than dofetilide.

To investigate the reason for the dependence of compound potency on the nature of the *para*-substituent, we determined the sensitivity of different substituents to mutations of pore (Thr-623, Ser-624, and Val-625) and S6 (Tyr-652 and Phe-656) helix residues (Fig. 6, A and B). The -fold change in potency induced by the double mutant T623A:S624A was greatest in the nitro compound and decreased as compound

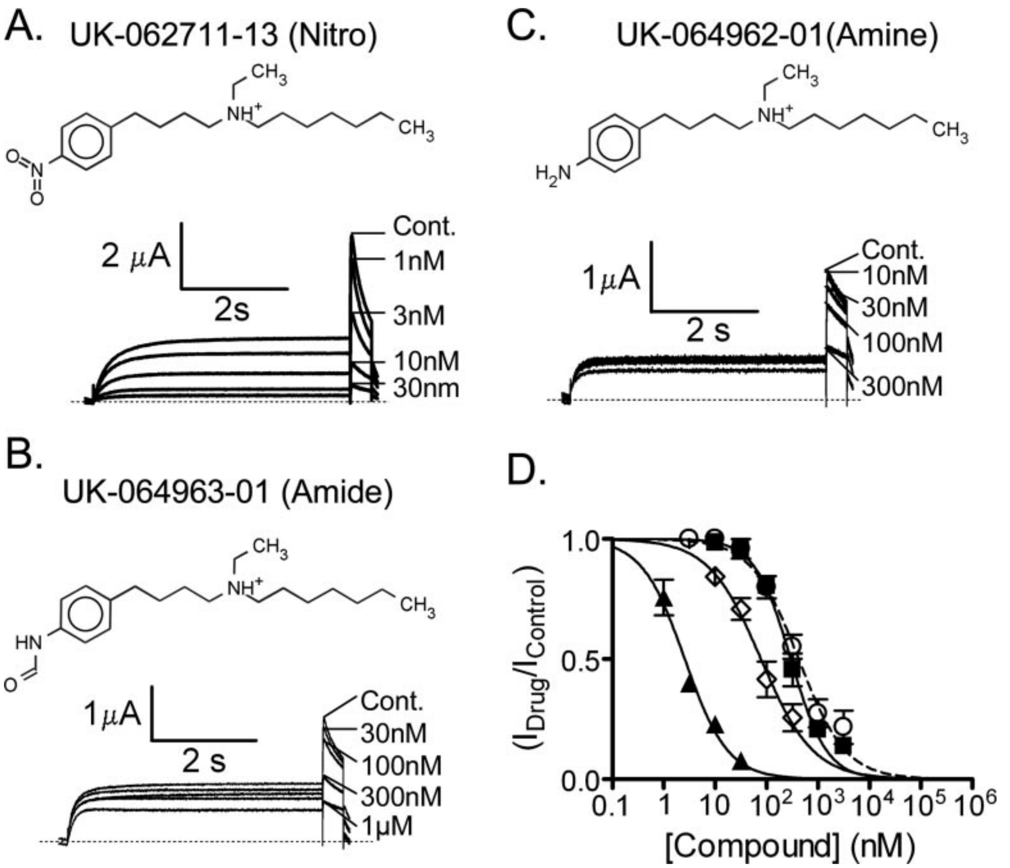

Fig. 5. Altering the phenyl ring *para*-substituent significantly alters compound potency. A to C, chemical structures of clofilium analogs (top). The analogs have a tertiary nitrogen and either nitro (A), amine (B), or amide (C) substituents at the *para*-position on the phenyl ring. Representative steady-state currents recorded from WT-hERG (bottom) are shown at a range of concentrations for each analog. D, concentration-response relationship for WT-hERG tail current block by tertiary clofilium analogs with either chlorine (PNU-0068611A, ◇), nitro (UK-062711–13, ▲), amine (UK-064962–01, ■), or amide (UK-064963–01, ○) at the *para*-position on the phenyl ring. IC_{50} values are shown in Table 3.

potency to WT-hERG decreased (Fig. 6C). This further implicates two polar pore helix residues (Thr-623 and Ser-624) as sites of interaction with *para*-substituents of compounds and suggests that the differences in block by ibutilide and clofilium are due to properties of the *para*-substituent. Further mutational analysis of pore helix interactions was not possible because mutations were not tolerated. We were unable to obtain functional expression of Val, Leu, Ile, Cys, Lys, Tyr, and Asn mutants at positions 623 and 624. With the exception of V625A, mutations of Val-625 were also nonfunctional. These residues are highly conserved in K^+ channels (Shealy et al., 2003). They are clearly required for normal function of the selectivity filter.

TABLE 2

IC_{50} values for WT-hERG tail current inhibition by dofetilide and four analogs that differ only in the *para*-substituents

Compound	Structure	IC_{50}	*n*
		nM	
Dofetilide	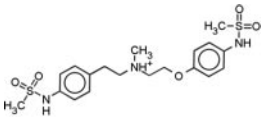	47.3 ± 4	8
UK-068522	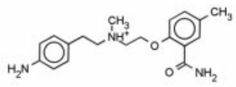	2590 ± 280	7
UK-068523	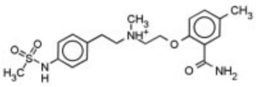	81 ± 25	5
UK-068526-01	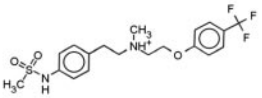	44 ± 6	7
UK-068097	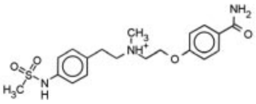	922 ± 170	7

Mutation of S6 helix residues Tyr-652 and Phe-656 to Ala greatly reduced sensitivity to block by all four *para*-substituent analogs (Table 3). The -fold reduction in potency was similar for chlorine, amine, and amide analogs on both Y652A (129- to 193-fold) and F656A (420- to 422-fold) hERG channels. However, much larger shifts in IC_{50} were observed with the nitro- compound on Y652A (1833-fold) and F656A (2688-fold) hERG channels. Therefore, the most potent compound for WT-hERG block (at least 20-fold more potent than the chlorine-containing compound) also exhibited the greatest decrease in potency with Y652A and F656A (Fig. 6D).

The relationship between the potency of each compound and the -fold shift in IC_{50} induced by alanine mutations of the pore and S6 helix residues is shown in Fig. 7. Good correlation exists between potency on WT-hERG and -fold-shifts induced by T623A:S624A and Y652A, suggesting that interactions with these residues play a particularly important role in high-affinity binding.

Discussion

Permanent Positive Charge on Clofilium Confers Slow Kinetics of Block, without Affecting Recovery from Block or hERG Binding Site Interactions. Ultraslow kinetics for the onset of K^+ channel block by quaternary clofilium has previously been reported in *X. laevis* oocytes

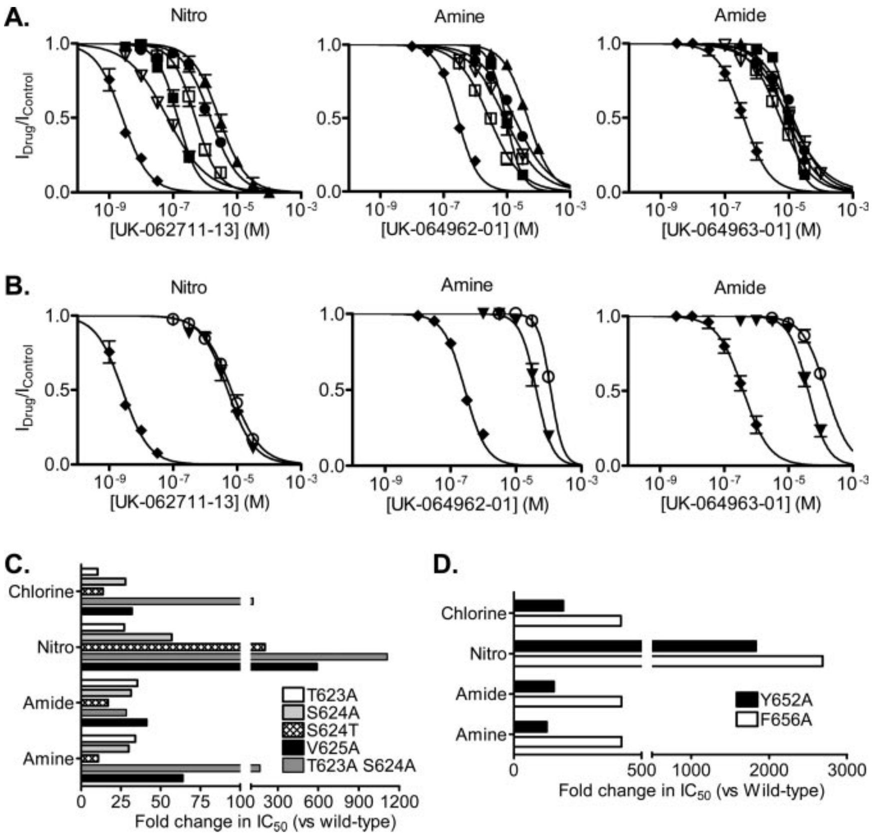

Fig. 6. Differential sensitivity of pore and S6 helix mutants to block by clofilium analogs. A and B, mean concentration-response relationships for block of pore (A) and S6 (B) helix mutant channels by nitro, amine, and amide clofilium analogs. ♦, WT; ▽, T623A; ■, S624A; □, S624T; ●, V625A; ▲, T623A:S624A; ○, F656A; ▼, Y652A. Standard errors are not shown if bars are smaller than data symbol. IC_{50} values are shown in Table 3. C and D, -fold changes in IC_{50} values for each pore (C) and S6 (D) helix mutant relative to WT hERG.

(Suessbrich et al., 1997; Steidl and Yool, 2001; Perry et al., 2004), mammalian cell lines (Gessner and Heinemann, 2003), and rat ventricular myocytes (Castle, 1991). As predicted, the slow kinetics of block were not observed with the tertiary clofilium compound PNU-0068611A, which differs from clofilium only in the removal of an ethyl group from the central quaternary nitrogen and the addition of a benzylic hydroxyl group (Fig. 1). The hydroxyl is unlikely to contribute to the rapid onset of block because similar rapid kinetics were observed with other tertiary clofilium analogs in which it is absent. Slow equilibration across the membrane due to the permanent positive charge of clofilium is most likely responsible for the slow onset of block.

Clofilium and PNU-0068611A differ by only 2-fold in their potency for WT-hERG block. However, the potency of extracellularly applied quaternary clofilium is probably an underestimation of binding affinity as a result of slow and incomplete equilibration across the membrane in the whole-cell configuration. Indeed, clofilium block of hEAG1 channels is faster and the IC_{50} much lower when applied to the intracellular side of channels in excised patches (Gessner and Heinemann, 2003). Thus, it is likely that clofilium has a significantly higher potency for WT-hERG block than the tertiary compound. Unfortunately, hERG current rundown from excised inside-out patches is too rapid to determine the IC_{50} of drugs applied to the intracellular side of channels (M. Chang and J. Mitcheson, unpublished observations; also conclusion of Gessner and Heinemann, 2003). Our mutagenesis results indicate that both compounds share the same binding sites on hERG but shifts in IC_{50} were much greater for clofilium. Thus, small changes in compound structure—such as the addition of an ethyl group or removal of a hydroxyl group—can optimize inner cavity binding site interactions and thereby increase potency.

Slow recovery from clofilium block is not caused by a protonated, charged amine group because the tertiary compound unbinds with a slow rate similar to that of clofilium. Thus, in contrast to classic experiments on block of sodium channels by anesthetics (Hille et al., 1977; Hondeghem and Katzung, 1977), there is no evidence of hydrophilic pathways through which uncharged drug molecules could escape from the inner cavity of hERG.

***para*-Substituents Interact with Pore Helix Residues.** A large number of structurally diverse compounds have a high affinity for hERG. Structural features that are common to many are one or more phenyl rings and a charged central nitrogen 5.2 to 9.1 Å apart separated by a carbon atom linker (Cavalli et al., 2002; Ekins et al., 2002; Pearlstein et al., 2003). In this study, we show that the *para*-substituent on the phenyl ring of clofilium can also substantially influence drug potency. There was a shift of more than 100-fold in IC_{50} in the limited range of analogs we studied. Of the four tertiary analogs we tested, the rank order of potency against WT-hERG upon modifying the *para*-substituents was nitro > chlorine > amine > amide. Therefore, analogs with polar or electronegative *para*-substituents are more potent than those with neutral moieties. Similar results were obtained using a range of dofetilide analogs (Table 2), indicating that these findings were not restricted to clofilium analogs. It is noteworthy that Cavalli et al. (2002) high-

TABLE 3

IC_{50} values for WT and mutant hERG current inhibition by four tertiary clofilium analogs with the indicated *para*-substituents on the phenyl ring

ΔIC_{50} represents the -fold shift in IC_{50} of each mutant channel compared to WT-hERG.

Mutation	Nitro UK-062711–13		Amine UK-064962–01		Amide UK-064963–01		Chlorine PNU-0068611A	
	IC_{50}	ΔIC_{50}	IC_{50}	ΔIC_{50}	IC_{50}	ΔIC_{50}	IC_{50}	ΔIC_{50}
	μM		*μM*		*μM*		*μM*	
WT	0.003 ± 0.05		0.273 ± 0.02		0.329 ± 0.09		0.081 ± 0.02	
T623A	0.068 ± 0.01	27	9.284 ± 1.76	34	11.68 ± 3.18	36	0.845 ± 0.26	11
S624A	0.143 ± 0.02	57	8.206 ± 2.21	30	10.33 ± 1.33	32	2.263 ± 0.42	28
S624T	0.517 ± 0.10	207	2.958 ± 0.47	11	5.580 ± 0.68	17	1.117 ± 0.19	14
T623A:S624A	2.784 ± 0.29	1110	45.66 ± 2.14	167	9.380 ± 1.38	29	9.406 ± 1.80	116
V625A	1.481 ± 0.23	591	17.49 ± 2.80	64	13.57 ± 1.00	41	2.590 ± 0.22	32
Y652A	4.594 ± 0.56	1833	43.13 ± 6.27	158	42.64 ± 5.08	129	15.59 ± 1.30	193
F656A	6.738 ± 0.80	2688	115.1 ± 6.52	421	138.8 ± 12.5	422	33.96 ± 8.90	420

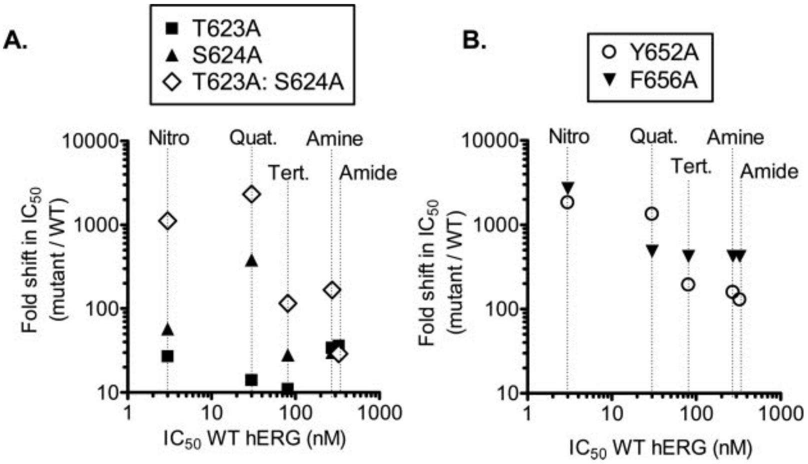

Fig. 7. -Fold shifts in IC_{50} induced by T623A:S624A and Y652A mutations correlate well with compound potency in WT-hERG. A and B, for each clofilium analog; -fold shifts in IC_{50} values (relative to WT-hERG) induced by pore (left) and S6 (right) mutations are plotted against the corresponding WT-hERG IC_{50} value. For T623A:S624A and Y652A, there is a reasonable relationship between these values, suggesting that these residues make an important contribution to binding interactions.

lighted polar (e.g., methanesulfonamides or nitro moieties) or polarizable (halogen atoms such as chlorine) regions in close proximity to the primary phenyl ring in their three-dimensional quantitative structure-activity relationship model of hERG channel blockers. It is possible that modifying the nature of the *para*-substituent could be a viable strategy for reducing hERG potency and liability to cause QT prolongation.

Of the hERG channel mutations tested, a good correlation between -fold change in IC_{50} and potency of *para*-substituent analogs for WT-hERG block was obtained with the double mutant T623A:S624A. In fact, this mutant shifted (impaired) the IC_{50} of the nitro- analog by approximately 1000-fold, indicating the importance of these residues for drug interactions. Therefore, we propose that the increased potency of compounds with polar *para*-substituents is caused by an enhanced affinity with the polar residues (Thr-623 and Ser-624) that face the inner cavity of hERG from the base of the pore helix. In addition, mutation of Tyr-652 (but not Phe-656) on the S6 helix also showed good correlation, suggesting that a combination of these two sites is important for high-affinity block.

In Silico Modeling. The hERG-ligand complexes produced by our docking studies seem to be consistent with the experimental results, thus aiding interpretation of the data at the atomic level. The apparent optimal binding mode for the ligand structures—adopted by all but ibutilide and the amide analog—is illustrated by the nitro analog in Fig. 8. In this mode, the *para*-substituent interacts with both Thr-623 and Ser-624 in the top corner of the cavity, whereas the phenyl ring is located where it may form a weak π-stacking interaction with the aromatic ring of Tyr-652. It is noteworthy that, in accordance with a previous report (Perry et al., 2004), this binding mode—particularly access to the top corner of the cavity—would be impeded by the additional methyl group of the G648A mutant. In addition, the protonated central nitrogen sits central to the cavity, roughly 5 Å from all four Tyr-652 aromatic rings, with which it is predicted to form cation-π interactions. Consistent with these findings, mutating Tyr-652 to a range of amino acids indicated that the aromaticity of the residue in this position is important for high-affinity block (Fernandez et al., 2004). The ethyl groups attached to the central nitrogen may also form hydrophobic interactions with Tyr-652. The second ethyl group of clofilium may contribute an additional hydrophobic interaction with one of the Y652 side chains, making it more sensitive to the Y652A mutation than the tertiary analog.

Ser-624, located at the C-terminal end of the pore helix, is an important site of interaction with clofilium. Mutation of Ser-624 to Ala substantially reduced hERG block and facilitated recovery from block. However, S624A caused much smaller shifts in IC_{50} compared with the T623A:S624A double mutation. Our model predicts that despite their close spatial proximity, the hydroxyl group of Ser-624 is more optimally positioned than that of Thr-623 for interacting with the chlorine of clofilium. Indeed, in some of the other models generated (i.e., not the lowest energy model) Thr-623 is not pointing into the cavity. The hydroxyl group on Thr-623 may only be in a position to interact with clofilium when Ser-624 is mutated. We propose that the chlorine atom of clofilium can interact with the polar hydroxyl group of either residue but that a more specific high-affinity interaction occurs with Ser-624, possibly because of optimal positioning of this residue. The side chain of Val-625 is shielded from the inner cavity and is therefore not implicated in binding any of the compounds. Its side chain performs an important packing role behind the selectivity filter. The V625A mutant has modified ion selectivity and inactivation properties, suggesting that it affects drug binding indirectly.

The docking results suggest that increasing the length of the *para*-substituent—as in ibutilide and the amide analog—prevents such molecules from adopting the same orientation

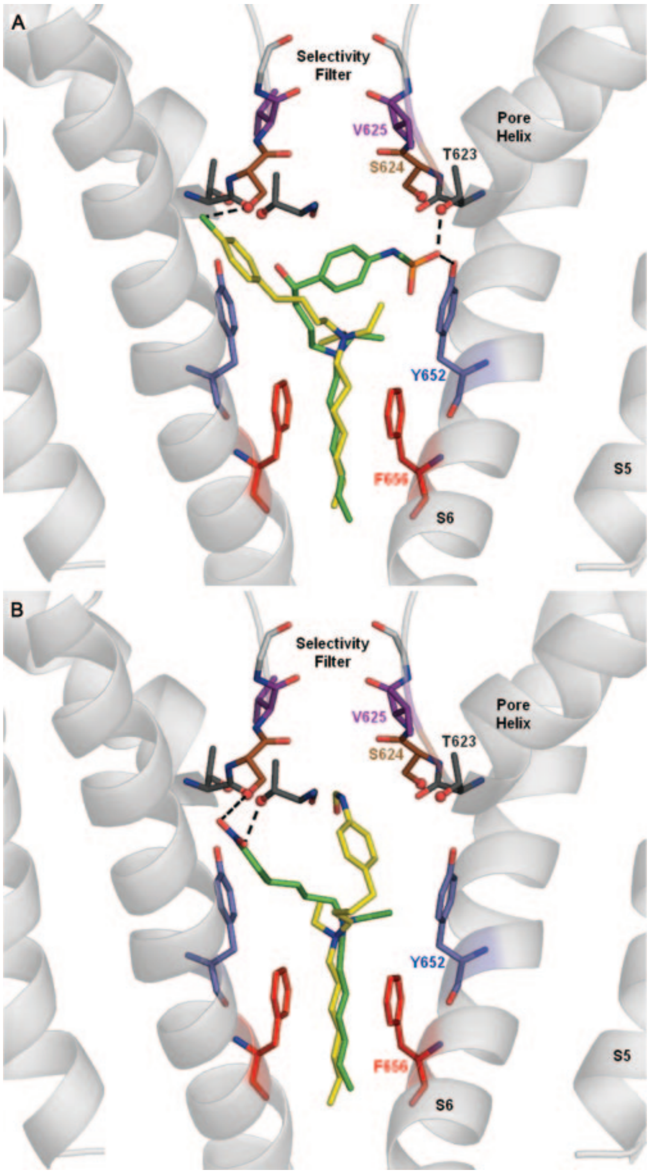

Fig. 8. A cross-section through the hERG model, viewed perpendicular to the cell membrane, illustrating the predicted binding to the central cavity of hERG of clofilium (yellow) and ibutilide (green) (A), and the nitro (green) and amide (yellow) clofilium analogs (B). The oxygen atoms of the hydroxyl groups of Thr-623 and Ser-624 are shown as spheres. Black dashed lines depict predicted hERG-ligand hydrogen bonds. The hydrophobic tails of all four compounds are shown to interact with Phe-656, whereas the phenyl ring of all but the amide analog is in a position to π-stack against Tyr-652. This predicted π-stacking interaction places the *para*-substituent in a suitable position to interact with hydroxyl side chains of both Thr-623 and Ser-624. For clarity, only two of the four subunits of hERG are shown. In the case of ibutilide, the Tyr-652 residue that π-stacks with the drug is not depicted.

as the nitro analog (Fig. 8B). The modeling results suggest that ibutilide can compensate for the increase in size by adopting an alternative favorable binding mode. In this configuration, the methanesulfonamide (the *para*-substituent of ibutilide) also resides in the top corner of the cavity, suggestive of interactions with both Thr-623 and Ser-624. In this binding mode, an interaction is predicted between the sulfonyl group of ibutilide and the side-chain hydroxyl of Tyr-652. In addition, the phenyl ring of ibutilide is predicted to π -stack with another Tyr-652 in an edge-on-face interaction. A further hydrogen bond may also form between the hydroxyl group, one carbon away from the phenyl in ibutilide, and the side chain of Ser-624 (Fig. 8A). The amide analog, lacking both the sulfonyl and hydroxyl groups of ibutilide, seems to be unable to adopt this orientation and interacts with neither Thr-623 nor Ser-624, with the nitrogen of its *para*-substituent binding centrally, at the intracellular mouth of the selectivity filter. The interactions with Tyr-652 are also limited (Fig. 8B). This is consistent with the lower affinity of the amide analog.

In all cases, the hydrophobic tail rests between all four Phe-656 residues (one from each subunit). Consistent with the finding that hydrophobicity, rather than aromaticity, of the residue at the position corresponding to Phe-656 was important for drug binding (Fernandez et al., 2004). A hydrophobic interaction may exist between the tail of the drug and a "hydrophobic basket" formed at the base of the inner cavity by four Phe-656 residues and four Val-659 residues. Because the hydrophobic tail region of the compound does not change between quaternary and tertiary clofilium analogs, this explanation is supported by the identical shifts in affinity observed with F656A mutation between the two analogs.

There are a number of limitations to the study that should be taken into consideration. First, we measure current inhibition to investigate drug interactions, rather than measuring ligand binding directly. As mentioned previously, our measurements are influenced by factors such as membrane permeability that affect the free, intracellular concentration of drug. The potency of compounds in *X. laevis* oocytes is usually lower than in mammalian cells, possibly because drug is absorbed by the yolk sack. Second, mutations of specific amino acids may alter drug block through an allosteric effect on the binding site. This is very likely to be the reason that the V625A mutant reduces drug sensitivity. Third, structural differences within a compound series may alter drug properties such as lipophilicity and membrane permeability. We have minimized this by using very close analogs with CLogP values that differ by less than 1 log unit. Finally, we have used in silico docking studies to help visualize drug interactions and interpret our experimental findings. The modeling presented herein is based upon a closed-state model of hERG. Current models are restricted by the lack of a crystal structure for hERG and because the dynamic conformational activities of the channel are not taken into account with the docking methods used. Nevertheless, the combination of mutagenic, electrophysiological, and computational techniques has proved valuable for understanding hERG channel block.

In summary, our results indicate that specific alterations in drug structure significantly altered the potency for block of WT-hERG channels. For instance, changing the *para*-substituent of clofilium analogs from polar to neutral reduced potency 100-fold. This was due to lower affinity interactions with pore (Thr-623 and Ser-625) and S6 (Tyr-652) helix residues. Molecular modeling provides an interpretation at the atomic level for the experimental data and further emphasizes the importance of pore helix residue interactions with the *para*-substituents of clofilium analogs. Our findings are likely to be applicable to many compounds and have important implications for the development of new drugs. Altering the *para*-substituent to reduce hERG binding could be highly beneficial if the efficacy against the primary target can also be maintained. Thus modifying the *para*-substituent could be a valuable strategy for reducing undesirable long QT side effects.

Acknowledgments

We thank Mr. Seung-Ho Kang for valuable technical assistance.

References

Berman HM, Westbrook J, Feng Z, Gilliland Feng, Bhat TN, Weissig H, Shindyalov IN, and Bourne PE (2000) The Protein Data Bank. *Nucleic Acids Res* **28:**235–242.

Castle NA (1991) Selective inhibition of potassium currents in rat ventricle by clofilium and its tertiary homolog. *J Pharmacol Exp Ther* **257:**342–350.

Cavalli A, Poluzzi E, De Ponti F, and Recanatini M (2002) Toward a pharmacophore for drugs inducing the long QT syndrome: insights from a CoMFA study of HERG K+ channel blockers. *J Med Chem* **45:**3844–3853.

Chen J, Seebohm G, and Sanguinetti MC (2002) Position of aromatic residues in the S6 domain, not inactivation, dictates cisapride sensitivity of HERG and eag potassium channels. *Proc Natl Acad Sci USA* **99:**12461–12466.

Doyle DA, Morais Cabral J, Pfuetzner RA, Kuo A, Gulbis JM, Cohen SL, Chait BT, and MacKinnon R (1998) The structure of the potassium channel: molecular basis of K^+ conduction and selectivity. *Science (Wash DC)* **280:**69–77.

Ekins S, Crumb WJ, Sarazan RD, Wikel JH, and Wrighton SA (2002) Three-dimensional quantitative structure-activity relationship for inhibition of human ether-a-go-go-related gene potassium channel. *J Pharmacol Exp Ther* **301:**427–434.

Fermini B and Fossa AA (2003) The impact of drug-induced QT interval prolongation on drug discovery and development. *Nat Rev Drug Disc* **2:**439–447.

Fernandez D, A Ghanta, GW Kauffman, and MC Sanguinetti (2004) Physicochemical features of the HERG channel drug binding site. *J Biol Chem* **279:**10120–10127.

Ficker E, Jarolimek W, and Brown AM (2001) Molecular determinants of inactivation and dofetilide block in ether a-go-go (EAG) channels and EAG-related K^+ channels. *Mol Pharmacol* **60:**1343–1348.

Gessner G and Heinemann SH (2003) Inhibition of hEAG1 and hERG1 potassium channels by clofilium and its tertiary analogue LY97241. *Br J Pharmacol* **138:** 161–171.

Gessner G, Zacharias M, Bechstedt S, Schonherr R, and Heinemann SH (2004) Molecular determinants for high-affinity block of human EAG potassium channels by antiarrhythmic agents. *Mol Pharmacol* **65:**1120–1129.

Herzberg IM, Trudeau MC, and Robertson GA (1998). Transfer of rapid inactivation and sensitivity to the class III antiarrhythmic drug E-4031 from HERG to M-eag channels. *J Physiol* **511:**3–14.

Hille B (1977) Local anesthetics: hydrophilic and hydrophobic pathways for the drug-receptor reaction. *J Gen Physiol* **69:**497–515.

Hondeghem LM and Katzung BG (1977). Time- and voltage-dependent interactions of antiarrhythmic drugs with cardiac sodium channels. *Biochim Biophys Acta* **472:**373–398.

Jones G, Willett P, Glen RC, Leach AR, and Taylor R (1997) Development and validation of a genetic algorithm for flexible docking. *J Mol Biol* **267:**727–748.

Kamiya K, Mitcheson JS, Yasui K, Kodama I, and Sanguinetti MC (2001) Open channel block of HERG K^+ channels by vesnarinone. *Mol Pharmacol* **60:**244–253.

Keating MT and Sanguinetti MC (2001) Molecular and cellular mechanisms of cardiac arrhythmias. *Cell* **104:**569–580.

Lees-Miller JP, Duan Y, Teng GQ, and Duff HJ (2000) Molecular determinant of high-affinity dofetilide binding to HERG1 expressed in *Xenopus* oocytes: involvement of S6 sites. *Mol Pharmacol* **57:**367–374.

Milnes JT, Crociani O, Arcangeli A, Hancox JC, and Witchel HJ (2003) Blockade of HERG potassium currents by fluvoxamine: incomplete attenuation by S6 mutations at F656 or Y652. *Br J Pharmacol* **139:**887–898.

Mitcheson JS, Chen J, Lin M, Culberson C, and Sanguinetti MC (2000a) A structural basis for drug-induced long QT syndrome. *Proc Natl Acad Sci USA* **97:**12329–12333.

Mitcheson JS, Chen J, and Sanguinetti MC (2000b) Trapping of a methanesulfonanilide by closure of the hERG potassium channel activation gate. *J Gen Physiol* **115:**229–240.

Mitcheson JS and Perry MD (2003) Molecular determinants of high-affinity drug binding to HERG channels. *Curr Opin Drug Disc Dev* **6:**667–674.

Pearlstein RA, Vaz RJ, Kang J, Chen XL, Preobrazhenskaya M, Shchekotikhin AE, Korolev AM, Lysenkova LN, Miroshnikova OV, Hendrix J, et al. (2003) Characterization of HERG potassium channel inhibition using CoMSiA 3D QSAR and homology modeling approaches. *Bioorg Med Chem Lett* **13:**1829–1835.

Perry M, de Groot MJ, Helliwell R, Leishman D, Tristani-Firouzi M, Sanguinetti

MC, and Mitcheson J (2004) Structural determinants of HERG channel block by clofilium and ibutilide. *Mol Pharmacol* **66:**240–249.

Recanatini M, Poluzzi E, Masetti M, Cavalli A, and De Ponti F (2004) QT prolongation through hERG K$^+$ channel blockade: current knowledge and strategies for the early prediction during drug development. *Med Res Rev* **25:**133–166.

Sali A and Blundell TL (1993) Comparative protein modelling by satisfaction of spatial restraints. *J Mol Biol* **234:**779–815.

Ridley JM, Milnes JT, Witchel HJ, and Hancox JC (2004) High affinity HERG K(+) channel blockade by the antiarrhythmic agent dronedarone: resistance to mutations of the S6 residues Y652 and F656. *Biochem Biophys Res Commun* **325:**883–891.

Sanchez-Chapula J, Navarro-Polanco RA, Culberson C, Chen J, and Sanguinetti M (2002) Molecular determinants of voltage dependent HERG K$^+$ channel block. *J Biol Chem* **277:**23587–23595.

Sanchez-Chapula JA, Ferrer T, Navarro-Polanco RA, and Sanguinetti MC (2003) Voltage-dependent profile of human *ether-a-go-go*-related gene channel block is influenced by a single residue in the S6 transmembrane domain. *Mol Pharmacol* **63:**1051–1058.

Sanguinetti MC, Jiang C, Curran ME, and Keating MT (1995) A mechanistic link between an inherited and an acquired cardiac arrhythmia: HERG encodes the IKr potassium channel. *Cell* **81:**299–307.

Sanguinetti MC and Mitcheson JS (2005) Predicting drug-hERG channel interactions that cause acquired long QT syndrome. *Trends Pharmacol Sci* **26:**119–124.

Sanguinetti MC and Xu QP (1999). Mutations of the S4–S5 linker alter activation properties of HERG potassium channels expressed in Xenopus oocytes. *J Physiol* **514** (Pt 3): 667–75.

Shealy RT, Murphy AD, Ramarathnam R, Jakobsson E, and Subramaniam S (2003) Sequence-function analysis of the K$^+$-selective family of ion channels using a comprehensive alignment and the KcsA channel structure. *Biophys J* **84:**2929–2942.

Spector PS, Curran ME, Keating MT, and Sanguinetti MC (1996) Class III antiarrhythmic drugs block HERG, a human cardiac delayed rectifier K$^+$ channel. Open-channel block by methanesulfonanilides. *Circ Res* **78:**499–503.

Steidl JV and Yool AJ (2001) Distinct mechanisms of block of Kv1.5 channels by tertiary and quaternary amine clofilium compounds. *Biophys J* **81:**2606–2613.

Suessbrich H, Schonherr R, Heinemann SH, Lang F, and Busch AE (1997) Specific block of cloned Herg channels by clofilium and its tertiary analog LY97241. *FEBS Lett* **414:**435–438.

Tseng GN (2001) I$_{Kr}$: the hERG channel. *J Mol Cell Cardiol* **33:**835–849.

Vandenberg JI, Walker BD, and Campbell TJ (2001). HERG K$^+$ channels: friend and foe. *Trends Pharmacol Sci* **22:** 240–6.

Address correspondence to: John Mitcheson, University of Leicester, Department of Cell Physiology and Pharmacology, Maurice Shock Medical Sciences Building, University Road, Leicester, LE1 9HN, United Kingdom. E-mail: jm109@le.ac.uk